



**HAL**  
open science

## Radial variation of some wood properties in European beech

Delphine Jullien, Shengquan Liu, Caroline Loup, Tancreède Alméras, Joseph Gril, Bernard Thibaut

► **To cite this version:**

Delphine Jullien, Shengquan Liu, Caroline Loup, Tancreède Alméras, Joseph Gril, et al.. Radial variation of some wood properties in European beech. 2024. hal-04133248v3

**HAL Id: hal-04133248**

**<https://hal.science/hal-04133248v3>**

Preprint submitted on 12 Aug 2024

**HAL** is a multi-disciplinary open access archive for the deposit and dissemination of scientific research documents, whether they are published or not. The documents may come from teaching and research institutions in France or abroad, or from public or private research centers.

L'archive ouverte pluridisciplinaire **HAL**, est destinée au dépôt et à la diffusion de documents scientifiques de niveau recherche, publiés ou non, émanant des établissements d'enseignement et de recherche français ou étrangers, des laboratoires publics ou privés.

# Radial variation of some wood properties in European beech

JULLIEN Delphine<sup>1</sup>, LIU Shengquan<sup>2</sup>, LOUP Caroline<sup>3</sup>,  
ALMERAS Tancredè<sup>1</sup>, GRIL Joseph<sup>4,5,\*</sup>, THIBAUT Bernard<sup>1</sup>

<sup>1</sup> LMGC, Univ Montpellier, CNRS, Montpellier, France

<sup>2</sup> School of Forestry & Landscape Architecture, Anhui Agricultural University, Hefei, China.

<sup>3</sup> Service du Patrimoine Historique, Univ Montpellier, Montpellier, France

<sup>4</sup> Université Clermont Auvergne, CNRS, Institut Pascal, Clermont-Ferrand, France

<sup>5</sup> Université Clermont Auvergne, INRAE, PIAF, Clermont-Ferrand, France

\* Corresponding author, email: [joseph.gril@cnrs.fr](mailto:joseph.gril@cnrs.fr)

## Keywords

Beech; Wood properties; Variability; Radial variation; Juvenile transition

## Abstract

The radial variation of wood properties, especially within the juvenile transition, exhibit patterns typical of the species, with, however, a strong dependence on growth conditions. Data obtained on beech (*Fagus sylvatica* L.) from several high forest stands in European countries have been revisited with a focus on this aspect. Laboratory measurements of ring width (*RW*), wood specific gravity (*SG*) and wood specific modulus (*SM*), were used to examine aspects of juvenility corresponding to young stages of the tree. The radial variations of *RW*, *SG* and *SM*, averaged over 86 trees, were close to the “typical radial pattern” of juvenile wood for softwood plantation trees: decrease in *RW* and increase in *SG* and *SM* from pith to bark in the juvenile phase. But *SG* only increased in the very first rings, then remained more or less constant. Furthermore, for all three parameters there were many discrepancies in the pattern of variation between trees and between plots. This is a good indication that the mechanical juvenility of the wood was more related to the mechanical conditions experienced by the trees in the young ages than to the age of the tree as such, as is the case for other features such as fibre length. Moreover, no significant influence of red heart occurrence on wood properties was observed.

## Notations and abbreviations

ANOVA analysis of variance

*CV* coefficient of variation

*D* density

*DP* distance to pith

*L, L* longitudinal direction, , specimen length in L direction

*MFA* microfibril angle

*MOE* modulus of elasticity

*R, R* radial direction, specimen length in R direction

*RW* ring width

*SG* specific gravity (ratio of *D* over water density)

*SM* specific modulus (ratio of *MOE* over *D*)

*T, T* tangential direction, specimen length in T direction

TRP typical radial pattern

*W* specimen weight

## 1. Introduction

45 Wood growth is the process used for tree building (Thibaut 2019) including simultaneously  
46 primary growth by elongation or creation of twigs and secondary growth by thickening of  
47 existing woody axes. The variation of growth parameters characterizing wood structure and  
48 properties depends on tree ontogeny and adaptation to changes in the environment of the tree  
49 during its life. Juvenility, in particular, describes the evolution of wood parameters during the  
50 early years of the stem. But the environment of the tree (access to light, wind influence, effect  
51 of gravity) also changes during the young period of tree growth and mechanical adaptation of  
52 wood growth occurs in response to these changes.

53 Secondary growth is performed by living wood cells in the cambial zone: stem cells of cambium  
54 itself and daughter cells (Raven et al 2007, Savidge 2003, Déjardin et al 2010, Thibaut 2019) It  
55 consists of the following successive steps: division of the cambium stem cells into daughter  
56 cells; expansion of daughter cells until the end of primary wall formation; thickening of the  
57 fibre (or tracheid) cell walls until the end of secondary wall formation; lignification of the whole  
58 cell wall, including the compound middle lamella; programmed fibre and vessel cell death.  
59 During this cambial activity mechanical wood features are achieved. They can be described by  
60 ring width, result of combined cell division and expansion, density expressing cell wall  
61 thickening, specific modulus determined by the cellulose micro-fibril organisation in the cell  
62 wall, and maturation strain resulting from the final polymerization of lignin and other  
63 macromolecular processes (Thibaut & Gril 2021). All secondary growth descriptors display  
64 spatial variation within a portion of trunk, in the 3 cylindrical directions: transversely across  
65 radii (Tar), around the perimeter (Ap) and longitudinally along the stem (Las), called variation  
66 “TarApLas” within the tree by Savidge (2003). These variations are linked either to the effect  
67 of cambial age (called juvenility) or to the adaptation of the wood growth to external conditions  
68 (climate, light availability, accidental leaning, etc.).

69 Variations around the perimeter in a given ring are related to a mechanical adaptation in the  
70 control of posture, i.e. oblique growth in a given direction (in the case of coppice or for the  
71 search of light) or progressive change of axis curvature, either to restore verticality after  
72 accidental inclination of the tree (Almérás et al 2005, Almérás and Clair 2016) or to change the  
73 orientation of the branches after the death of the apex (Loup et al 1991). The variations along  
74 the stem deals with primary growth: i) succession of connected zones and free-from-branching  
75 portions of the axis and ii) ageing of the terminal bud in the successive growth unit. Apart from  
76 the vicinity of the branching zones, the variations are rather slow (Savidge 2003). Radial  
77 variations, from pith to bark at a given height level can be divided in two types: i) intra-ring  
78 short distance changes mostly due to intra-annual climatic changes and ii) variations of mean  
79 intra-ring properties linked both to cambium ageing (juvenility) and to the adaptation of  
80 secondary wood growth to tree mechanics at each growth step (gravity and wind forces  
81 depending on tree slenderness and crown development). It is not easy to separate the effects of  
82 age per se (time since birth of cambium in the growth unit) and of the mechanical situation of  
83 the tree at different growth ages (light availability, wind protection).

84 The biggest variations in dimensions and environment for a given tree over time occur during  
85 the young ages, and so are the variations of wood properties showing higher radial gradients in  
86 the inner part of the axis, called juvenile wood or core wood depending on the authors  
87 (Lachenbruch et al 2011) and their opinion concerning the main influencing factor (juvenility  
88 or adaptation).

89 A good description is given in Bendtsen & Senft (1986) for a softwood and a hardwood.  
90 Loblolly pine (Fig. 1) is an example of the typical radial pattern (TRP) of juvenility  
91 (Lachenbruch et al 2011): i) initial increase of tracheid length, specific gravity (*SG*) and specific  
92 modulus (*SM*), initial decrease of ring width (*RW*) and microfibril angle (*MFA*); *MFA* variations

93 are closely, negatively related to those of *SM*. This is the general case in softwood plantation  
94 trees (Cown & Dowling 2015, Larson et al 2001).

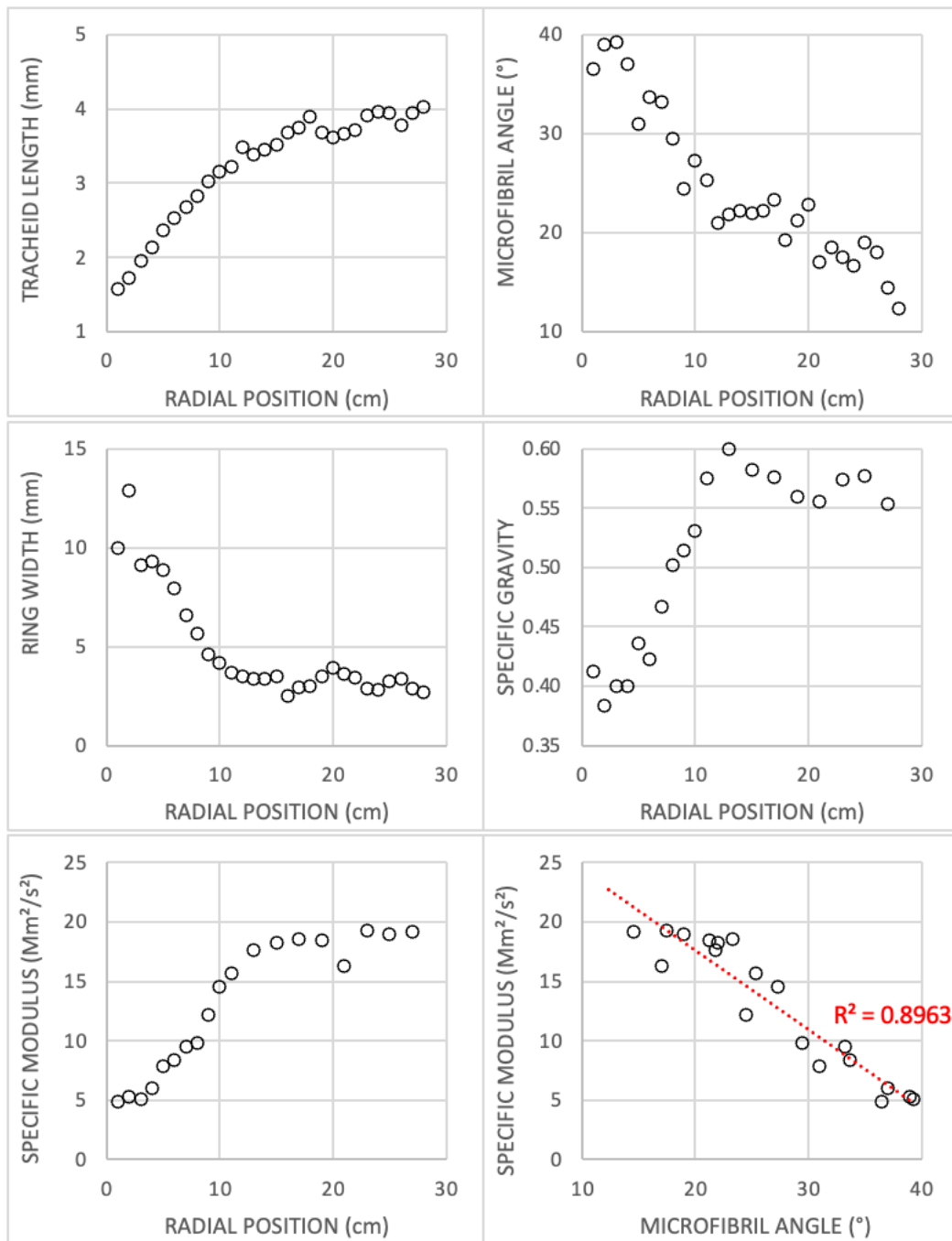


Fig. 1: Radial variations for Loblolly pine, after Bendtsen & Senft (1986).

95  
96  
97  
98

The same pattern applies to Eastern cottonwood (Fig. 2).

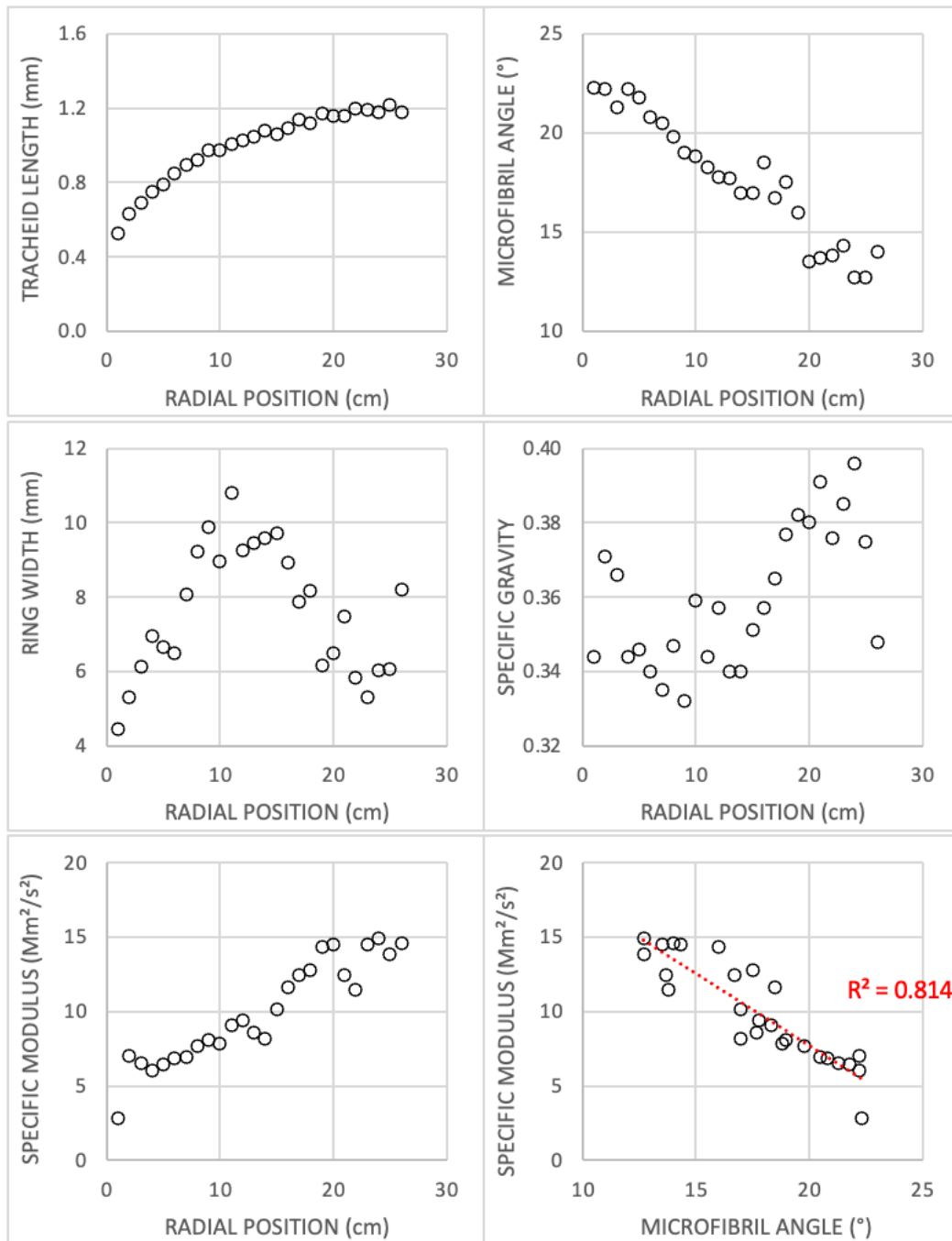


Fig. 2: Radial variations for Eastern cottonwood, after Bendtsen & Senft (1986).

99  
100  
101

102 Variations in tracheid or fibre length always share the same initial positive gradient for all trees,  
 103 whether softwood or hardwood (Koubaa et al 1998, Larson et al 2001, Bhat et al 2001, Bao et  
 104 al 2001, Kojima et al 2009). This parameter is important for the paper industry (Koubaa et al  
 105 1998) but is not cited as a factor influencing the mechanical properties of wood (Kollmann &  
 106 Côté 1968, Kretschman 2010). The results of initial variations of *RW*, *SG* and *SM* can vary  
 107 considerably from tree to tree, with flat, positive or negative initial gradients (Bhat et al 2001).  
 108 In this paper, the data obtained on a large panel of beech trees will be exploited to characterize  
 109 the patterns of radial variation of wood properties in beech. Beech wood has always the same  
 110 basic anatomy and chemical composition which are signatures of the species *Fagus sylvatica*  
 111 L. But within this physical and chemical pattern, quantitative variation occurs, linked to growth

112 adaptation to historical context (tree age, climate, forest management...) of the living tree at  
 113 the moment of the new layer forming.

114 Although heartwood and sapwood in healthy beech trees can scarcely be told apart, a referred  
 115 to as “red heartwood” is often observed (Liu et al 2005), with an inner distribution possibly  
 116 dependent on the presence of branch scars and knots (Wernsdörfer et al 2005) triggering the  
 117 massive arrival of oxygen (Sorz & Hietz 2008). Although technological properties do not seem  
 118 to be influenced by the discoloration (Pöhler et al 2006), it affects the commercial value of the  
 119 products (Trenčiansky et al 2017). Consequently, this factor will be also considered in the  
 120 analysis.

## 121 2. Material and methods

### 122 2.1. Material

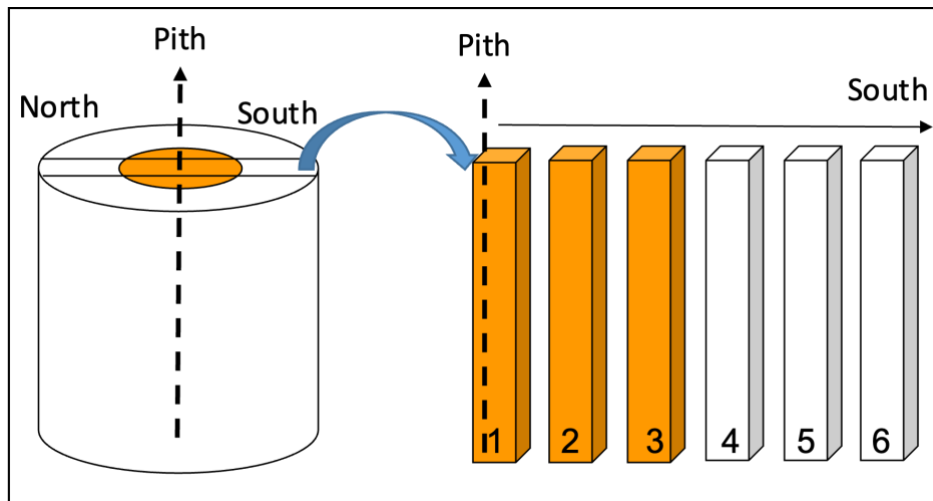
123 In nine plots representative of forest management in Western Europe (Becker & Beimgraben  
 124 2001, Jullien et al 2013), 10 trees (among 86 in total) were selected for the measurement of  
 125 wood properties. The types of management and plot ages are recalled in Table 1.

126  
 127 Table 1. Characteristics of the studied plots

Forest management	age (years)	Plot number								
		1	2	3	4	5	6	7	8	9
Classical even-aged forest, rather flat zone	100-130	o		o	o	o	o			
Classical even-aged forest, steep terrain (mountain)	120-150		o						o	
Uneven-aged high forest, rather flat zone	60-120							o		
Former middle forest later transformed in even-aged high forest	60									o
Country code		AT	AT	DK	FR	DE	DE	CH	CH	DE

128  
 129 One small log of 50 cm length was cut at a height of 4 m for each tree. Each small log was cut  
 130 into radial boards, through the pith, from North to South. These boards were air-dried to an  
 131 average moisture content of 13.5 % (equilibrium at 20°C and 65% RH) and cut into 1259 rods  
 132 of 20 mm in radial, 20 mm tangential and 360 mm longitudinal direction, from the pith outwards  
 133 (Fig. 3). Those with irregularities or cracks were discarded.

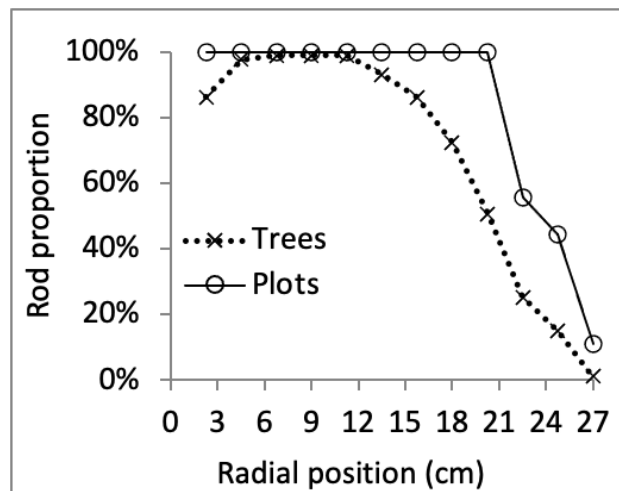
134 The rods were numbered according to their position in the board, their distance to pith (*DP*)  
 135 was measured, and their orientation (North or South) was noted. At the same time, the number  
 136 of rings at both ends of the samples was recorded and the mean annual ring width of the rod  
 137 (*RW*) was calculated as the ratio of the mean radial dimension to the number of rings. Each  
 138 sample located at a distance lower than 10 cm from the pith was considered as a “core” sample.  
 139 The presence of red heartwood was also noted for the rods located in the core, in relation to a  
 140 previously published work (Liu et al 2005).



141 Fig. 3: Diagram of the sawing of the rod after the sawing of a North-South diametrical board.  
 142  
 143 Numbering both for Northern and Southern parts of the board start with pith position. The coloured  
 144 parts evoke the case of redheart occurrence.

145 In each case, the occurrence of rods for each successive radial position within the trees or plots  
 146 was examined (Fig. 4). Up to 18 cm from the pith, all the plots were concerned and there were  
 147 always more than 70% of the trees concerned, values lower than 100% being due to defect  
 148 occurrence close to the pith. This proportion decreased rapidly for larger distances from the  
 149 pith, due to variable log size. It is therefore preferable not to use rods with a radial distance of  
 150 more than 18 cm to calculate the mean values of the parameters at the global scale.

141  
142  
143  
144  
145  
146  
147  
148  
149  
150  
151



152 Fig. 4 Percentage occurrence of rods for each successive radial position within trees or plots  
 153 100% means that there are used rods at a given radial position in every tree or every plot.  
 154

## 155 2.2. Measurement of properties.

156 All measurements were done in a regulated room at a temperature of 20°C and a relative  
 157 humidity of 65%.

158 The density ( $D$ ) was calculated by measuring the weight ( $W$ ) and the dimensions  $R$ ,  $T$ ,  $L$  of the  
 159 rod in direction  $R$ ,  $T$ ,  $L$ , respectively:  $D = W/(R.T.L)$ . The specific gravity ( $SG$ ) is the ratio  
 160 between  $D$  and water density.

161 To measure the specific modulus ( $SM$ ,  $10^6 m^2/s^2$ ), each rod is positioned on fine wires and set in  
 162 free vibration by a hammer stroke. The analysis of the sound vibration by fast Fourier transform  
 163 gives the values of the three highest resonance frequencies which are interpreted using

152  
153  
154  
155  
156  
157  
158  
159  
160  
161  
162  
163

164 Timoshenko solution (Brancheriau & Baillères 2002). The Young modulus of wood (*MOE*) can  
165 be calculated as:  $MOE = SG \cdot SM$ .

### 166 **2.3. Statistical analysis**

167 Basic statistical analyses were performed using XLSTAT software. The data description table  
168 includes the number of data, the minimum, maximum and mean values for each parameter, as  
169 well as the coefficient of variation (*CV*). The normality of the distribution is verified by Shapiro-  
170 Wilk test. A Pearson correlation analysis is used in the case of a normal distribution, and a  
171 Spearman correlation analysis in the case of a non-normal distribution, which is the majority of  
172 cases. Analysis of variance and variance components was carried out using the R software (R  
173 Core Team 2018), using a nested ANOVA design where a random “tree” factor is nested within  
174 the “plot” factor, and the “core” factor nested within the “tree” factor. Sample orientation (North  
175 or South) was accounted for through an independent “orientation” factor.

## 176 **3. Results**

### 177 **3.1 Analysis of variance and variance components**

178 ANOVA was highly statistically significant on each of the three measured variables (*RW*, *SG*  
179 and *SM*). Plot, tree within plot and core within tree were all very highly significant factors ( $P <$   
180  $10^{-16}$ ) for the three studied variables, while orientation is a significant factor only for specific  
181 modulus ( $P = 0.00012$ ). The share of variance of each factor for each variable is displayed in  
182 Table 2. For *RW*, the core factor represents the largest part of variance, followed by the plot and  
183 tree factors. For *SG* and *SM*, the tree factor is the largest part of variance. The orientation factor  
184 always represents a negligible part of variance, even when it is statistically significant (*SM*).

185

186 Table 2. Results of the variance component analysis: share of variance for each factor (%) and  
187 significance of the factors (\*\* $P < 10^{-3}$ , °  $P > 0.05$ )

Factor	RW	SG	SM
Plot	21.9***	14.0***	15.4***
Plot/tree	9.2***	36.4***	28.6***
Plot/tree/core	29.5***	18.2***	14.6***
Orientation	0.0°	0.0°	0.8***

188

### 189 **3.2. Radial variations of properties**

190 By giving positive values for the distance to the pith on the North side and negative values on  
191 the South side, it is possible to draw the South-North profile of each parameter (*RW*, *SG*, *SM*,  
192 *MOE*) for each tree, as a function of the diametrical position (*DP*). If there was an increase of  
193 the parameter from pith position, the profile is noted “Up”, “Down” for the reverse case and  
194 “Flat” when the variation was not clearly up or down. In case of clear asymmetry between the  
195 Southern and Northern parts by visual observation, the sample was considered as asymmetric  
196 (Fig. 5), otherwise it was noted as symmetric.

197



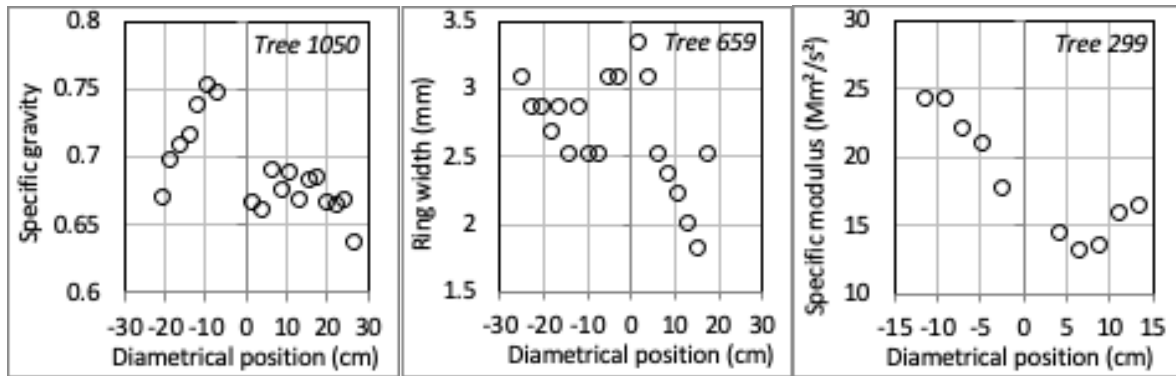


Fig. 5 Examples of clearly asymmetric North-South profiles.

There was a large majority of symmetrical patterns (Table 3).

Table 3 Proportion of profile types per plot within each wood parameter.

Para.	Ring width				Density				Specific modulus			
	Up	Down	Flat	Sym	Up	Down	Flat	Sym	PLOT	Up	Down	Flat
1	57%	43%	0%	70%	0%	25%	75%	40%	1	57%	43%	0%
2	67%	11%	22%	90%	11%	0%	89%	90%	2	67%	11%	22%
3	63%	0%	38%	80%	30%	0%	70%	100%	3	63%	0%	38%
4	70%	10%	20%	100%	20%	0%	80%	50%	4	70%	10%	20%
5	43%	14%	43%	70%	100%	0%	0%	60%	5	43%	14%	43%
6	86%	0%	14%	88%	50%	0%	50%	100%	6	86%	0%	14%
7	22%	56%	22%	90%	43%	14%	43%	70%	7	22%	56%	22%
8	67%	17%	17%	60%	100%	0%	0%	70%	8	67%	17%	17%
9	14%	57%	29%	88%	40%	0%	60%	63%	9	14%	57%	29%
Mean	54%	23%	23%	82%	44%	4%	52%	71%	Mean	54%	23%	23%

Para.: Wood parameter; Up: initial increase of the parameter from pith to bark; Down: initial decrease of the parameter from pith to bark; Flat: no clear initial increase or decrease; Sym: proportion of globally symmetrical profiles between North and South directions.

In accordance with the results of the variance component analysis, there were no noteworthy difference between the Northern and Southern samples (Table 4).

Table 4 Comparison of parameter values North and South.

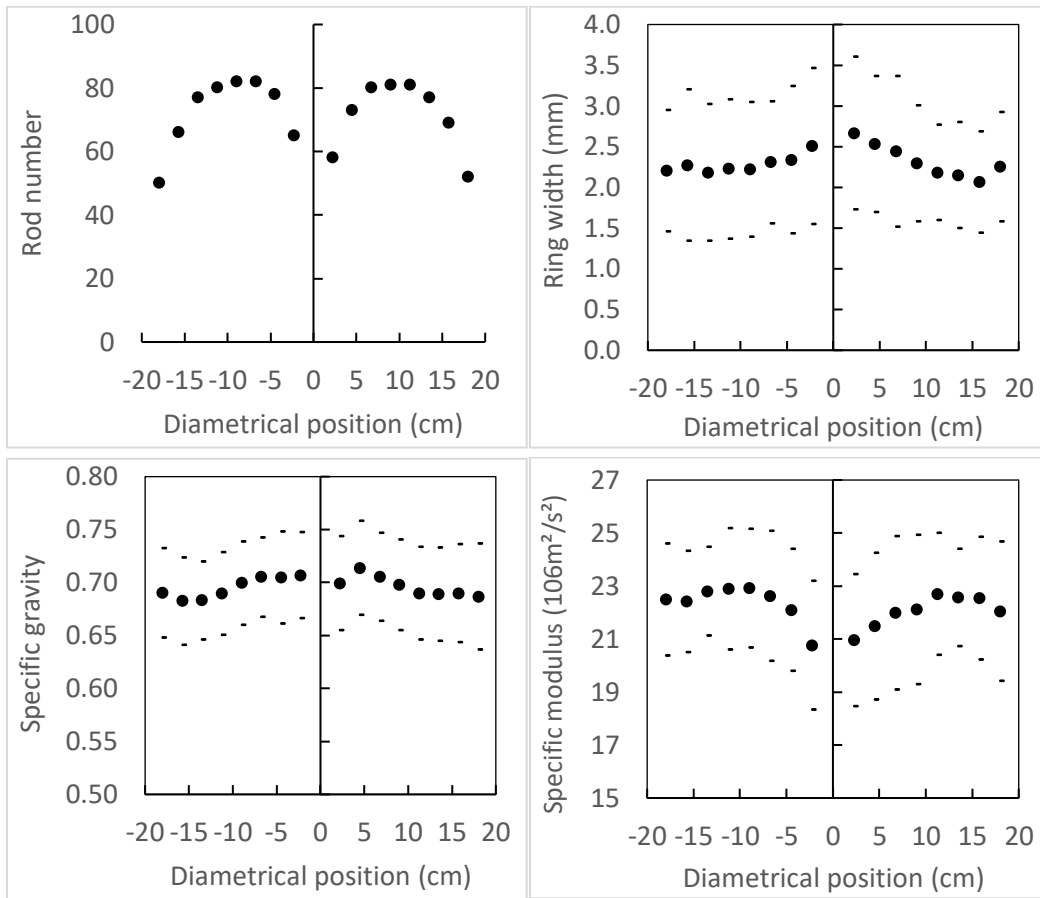
Position (Nb)	RW (mm)	SG	SM (10 <sup>6</sup> m <sup>2</sup> /s <sup>2</sup> )	MOE (GPa)
North (637)	2.32	0.695	22.06	15.33
South (622)	2.28	0.694	22.39	15.54
% Sym.	82%	71%	76%	70%

RW: mean ring width; SG: mean specific gravity; SM: mean specific modulus; MOE: mean longitudinal modulus of elasticity; Nb: number of rods; %Sym: proportion of diametrical patterns considered symmetrical for each parameter.

There were notable differences between trees for each parameter, both in value and in pattern. In Fig 6, the range of variation of the parameters values is given as a function of the position along the diameter, as well as the corresponding number of rods used for the calculation. There was no systematic difference between the Northern and Southern samples (Table 1, Fig. 6). It

219 was thus possible to mix the beech rods of the Northern and Southern specimens for further  
 220 analysis of the mean radial variation patterns at the global or plot level.

221



222

223

224

225

Fig. 6 Number of rods and parameter values for all trees as a function of diametrical position (DP)  
 Bolt dots: mean value; thin dashes: mean value + or – standard deviation.

226

227

228

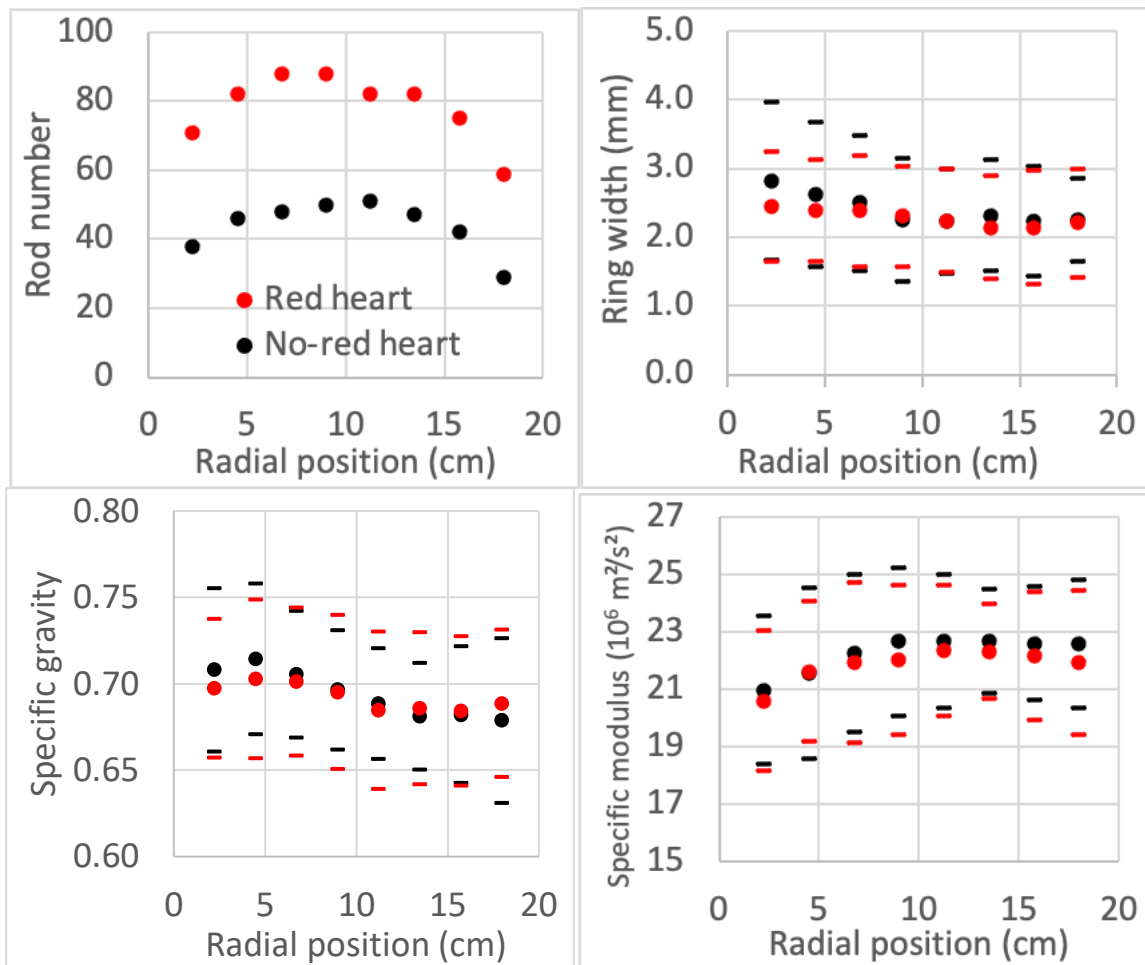
229

230

231

232

Moreover, some trees have a part of red core-wood portion and the effect it may have on  
 properties was investigated. All trees (25) without any red rod (except sometimes one near the  
 pith) were considered as white beech while all trees with more than two red rods were  
 considered as red beech. Fig. 7 shows the number of rods used for each radial position and the  
 mean radial variations of properties for red and white beech trees. Due to the variability between  
 the trees, no noteworthy difference could be observed between the mechanical properties of red  
 and white beech wood.



233

234  
235  
236  
237  
238

Fig. 7 Number of rods and parameter values for all red and no-red hearted trees as a function of radial position. Bolt dots: mean value; thin dashes: mean value + or – standard deviation.  
Red dots: red heartwood; black dots white heartwood

239 It is thus possible to mix Northern and Southern specimens of red and white beech rods for  
240 further analysis of the mean radial variation patterns at the global or plot level.

241 The global mean radial patterns for these beech trees were as follows (Fig. 8):

- 242 - *RW* decreases regularly (2.6 to 2.2 mm) from pith to bark;
- 243 - *SG* increases a little (0.703 to 0.709) at the beginning (up to about 4 cm radius) and  
244 decreases thereafter (0.709 to 0.686), but the variations are small;
- 245 - *SM* increases (20.8 to 22.8 m<sup>2</sup>/s) for a rather long time (up to about 12 cm radius) and then  
246 decreases (22.8 to 22.2 m<sup>2</sup>/s<sup>2</sup>) regularly;
- 247 - the *MOE* pattern is very similar to the *SM* pattern.

248

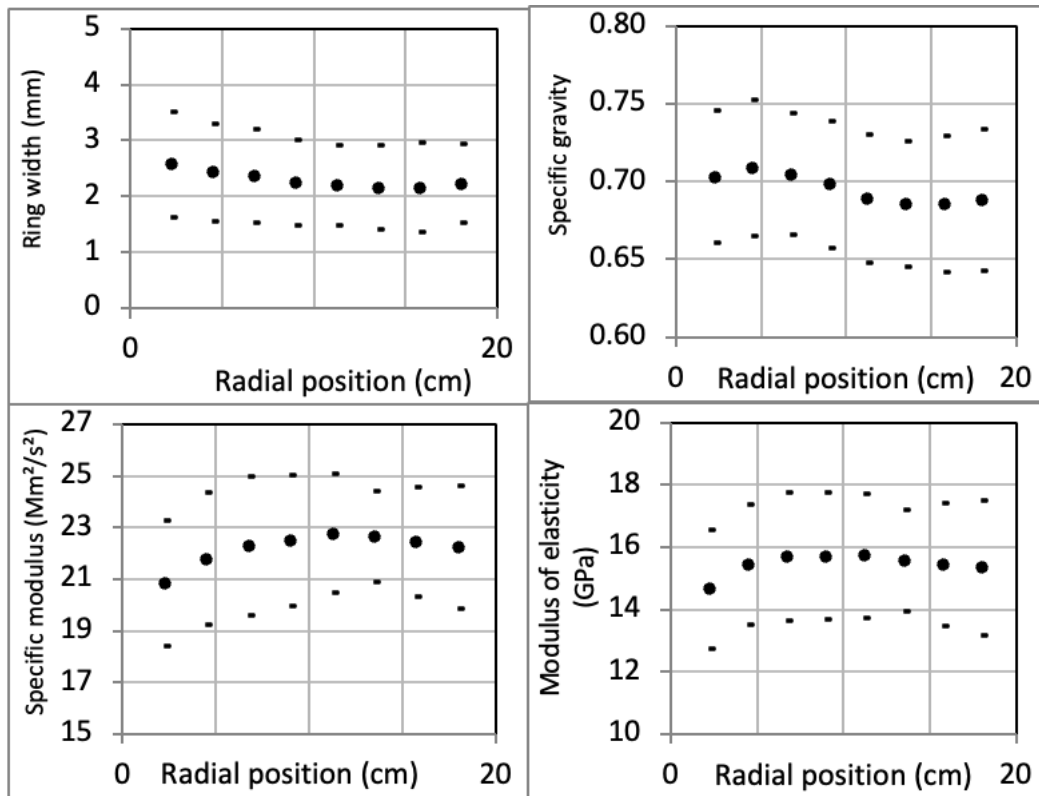
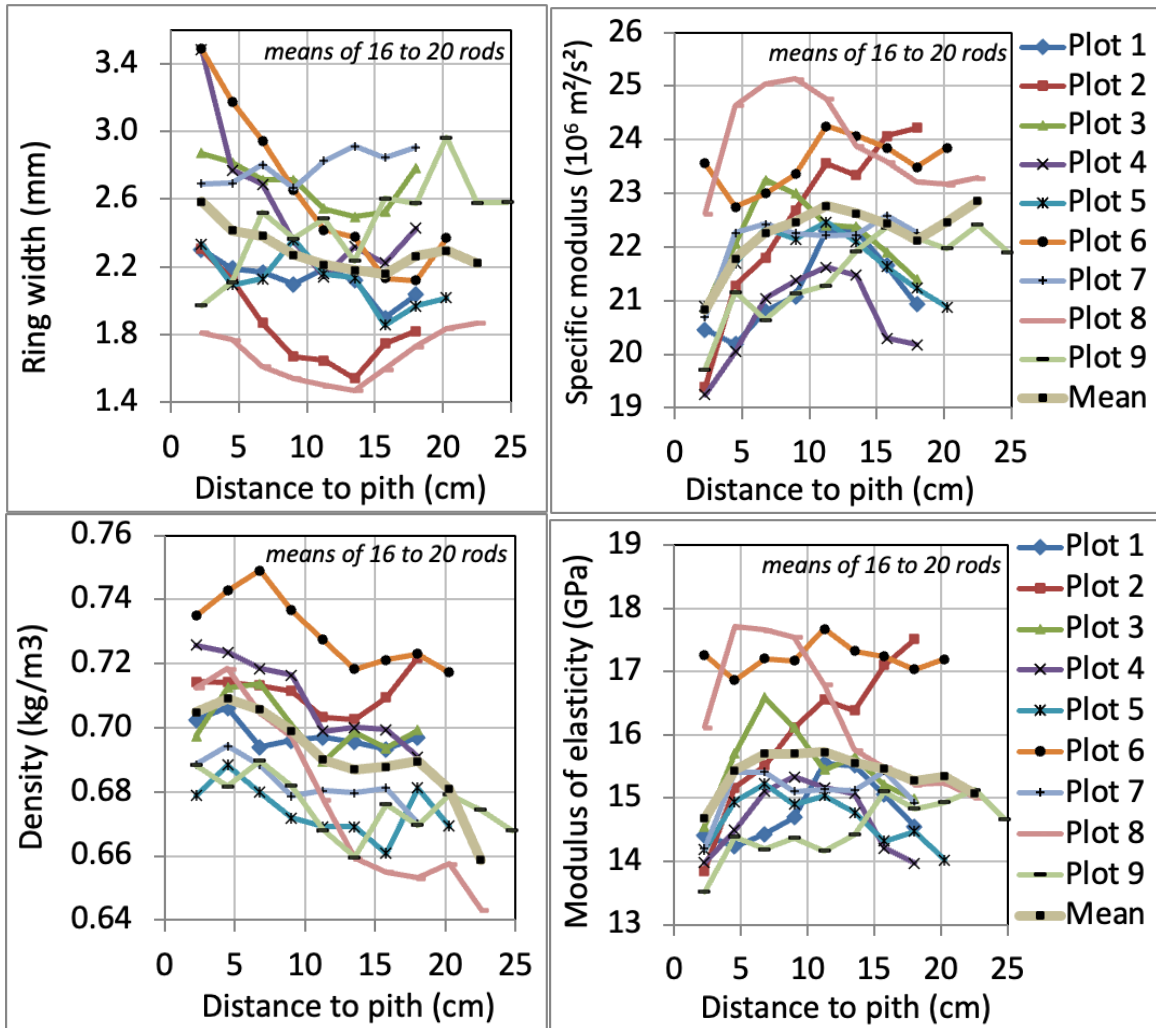


Fig. 8 Mean radial distribution of indicators and modulus of elasticity for all rods.  
 Bolt dots: mean value; thin dashes: mean value + or – standard deviation.

249  
 250  
 251  
 252  
 253  
 254  
 255  
 256  
 257  
 258  
 259

The variability between trees (coefficient of variation) is high for *RW* but low for *SG*. As will be seen later in Table 7, it is slightly higher for *SM* and *MOE*.  
 The mean patterns of the plots (Fig. 9) are more irregular due to the smaller number of rods, but the global mean pattern is the most frequent. There are differences between plots, in the mean level of properties and sometimes in the pattern, mainly for *RW*, with some plots having an increasing *RW* (plots 7 and 9). Others exhibit a decrease followed by an increase of *RW*, with low mean values (plots 2 and 8).

260



261

262

263

264

Fig. 9 Mean radial variations of properties at the plot level

Mean: mean values for all rods at each radial position. For plot characteristics, see Table 1

265 **3.3. Global results**

266 **3.4.1. Global results at rod level**

267 Table 5 and 6 give the global description and correlation within the data for all samples (1259  
 268 rods), respectively. The variation of *SG* between samples is very low (coefficient of variation  
 269 6%).

270

Table 5 Parameter description for all rods

1259 rods	<i>RW</i>	<i>SG</i>	<i>SM</i>	<i>MOE</i>
Minimum	0.67	0.55	11.08	8.00
Maximum	6.67	0.83	27.49	21.30
Mean	2.30	0.69	22.22	15.44
Max/min	10.00	1.51	2.48	2.66
Coefficient of variation	35.0%	6.2%	10.9%	13.0%

*RW* (mm): ring width; *SG*: specific gravity; *SM* ( $10^6 m^2/s^2$ ): specific modulus;  
*MOE* (GPa): longitudinal modulus of elasticity.

271

272

273

274

Table 6 Correlation table for all rods

1269 rods	<i>RW</i>	<i>SG</i>	<i>SM</i>	<i>MOE</i>
<i>RW</i>	<b>1</b>	<b>0.215</b>	<b>-0.313</b>	<b>-0.167</b>
<i>SG</i>		<b>1</b>	0.047	<b>0.506</b>
<i>SM</i>			<b>1</b>	<b>0.884</b>
<i>MOE</i>				<b>1</b>

275 *RW*: ring width; *SG*: specific gravity; *SM*: specific modulus; *MOE*: longitudinal modulus of elasticity.  
 276 Bold numbers: correlation significant at 0.01% level.  
 277

278 There is no significant correlation (at the 5% level) between *SG* and *SM*. *RW* has a very  
 279 significant correlation (at the 0.1% level) positively with *SG* and negatively with *SM*. Thus, the  
 280 correlation between *RW* and *MOE* is negative with a lower coefficient of determination (3%).  
 281 In the determination of *MOE* from *SM* and *SG*, the coefficient of determination (square of the  
 282 correlation coefficient given in Table 5) is three times higher for *SM* (78%) than for *SG* (26%).

283 3.4.2. Global results at tree level

284 Tables 7 and 8 give the description and correlation table for tree dimension and mean per tree.  
 285 Variability of parameters is significantly lower for tree mean values, and notably low for *SG*.  
 286 Except for *RW*, the mean wood properties per tree show rather low variations between trees  
 287 (very low for *SG*). Among the wood properties, *RW* and *SM*, *SM* and *MOE*, *SG* and *MOE* remain  
 288 highly significantly correlated (0.1% level) at the tree level.

289

290

Table 7 Parameter description for tree mean values

86 trees	<i>RW</i>	<i>SG</i>	<i>SM</i>	<i>MOE</i>
Minimum	1.29	0.63	17.6	12.0
Maximum	4.78	0.78	25.6	19.3
Mean	2.28	0.70	22.4	15.6
Max/min	3.70	1.24	1.46	1.60
Coefficient of variation	24.9%	4.8%	7.6%	9.5%

291 *RW* (mm): ring width; *SG*: specific gravity; *SM* ( $10^6\text{m}^2/\text{s}^2$ ): specific modulus;  
 292 *MOE* (GPa): longitudinal modulus of elasticity.  
 293

294

Table 8. Correlation table for all trees

86 trees	<i>RW</i>	<i>SG</i>	<i>SM</i>	<i>MOE</i>
<i>RW</i>	<b>1</b>	0.122	<b>-0.388</b>	-0.252
<i>SG</i>		<b>1</b>	0.140	<b>0.602</b>
<i>SM</i>			<b>1</b>	<b>0.874</b>
<i>MOE</i>				<b>1</b>

295 *RW*: ring width; *SG*: specific gravity; *SM*: specific modulus; *MOE*: longitudinal modulus of elasticity.  
 296 Bold numbers: correlation significant at 0.01% level.  
 297

298 3.4.3. Global results at plot level

299 Table 9 gives the description of tree dimensions and mean wood properties per tree for the 9  
 300 plots and Table 10 the correlation table for all plots. Except for *RW*, the mean wood properties  
 301 per plot all show very little variation between plots.  
 302

303

Table 9 Parameter description for the 9 plots mean values

Plot	Nb trees	<i>RW</i>	<i>SG</i>	<i>SM</i>	<i>MOE</i>
1	10	2.06	0.70	21.5	15.0
2	10	1.80	0.71	23.1	16.4
3	10	2.63	0.70	22.2	15.6
4	10	2.50	0.71	21.2	15.1
5	10	2.12	0.68	21.9	14.8
6	8	2.57	0.73	23.7	17.3
7	10	2.84	0.68	22.0	15.1
8	10	1.63	0.68	24.1	16.4
9	8	2.50	0.67	21.7	14.6
Max		2.84	0.73	24.1	17.3
Min		1.63	0.67	21.2	14.6
Mean		2.29	0.70	22.4	15.6
Max/min		1.74	1.08	1.14	1.18
Coefficient of variation		16.9%	2.6%	4.2%	5.5%

*RW* (mm): ring width; *SG*: specific gravity; *SM* ( $10^6\text{m}^2/\text{s}^2$ ): specific modulus;

*MOE* (GPa): longitudinal modulus of elasticity.

304

305

306

307 At the plot mean level, only the causal relationship between *MOE* and *SG* or between *MOE* and  
308 *SM* remains significant at the 0.1% level (Table 10).

309

310

Table 10. Correlation table for all plots

9 plots	<i>RW</i>	<i>SG</i>	<i>SM</i>	<i>MOE</i>
<i>RW</i>	<b>1</b>	0.154	-0.446	-0.266
<i>SG</i>		<b>1</b>	0.252	0.671
<i>SM</i>			<b>1</b>	<b>0.886</b>
<i>MOE</i>				<b>1</b>

311 *RW*: ring width; *SG*: specific gravity; *SM*: specific modulus; *MOE*: longitudinal modulus of elasticity.

312

Bold numbers: correlation significant at 0.1% level.

## 313 5. Discussion

314 Most of the papers on juvenile wood refer to plantation, either of softwoods or hardwoods  
315 (Bensend and Senft 1986, Kojima et al 2009, Bhat et al 2001, Bao et al 2001). Fibre length  
316 which is not referred as a mechanical factor (Kretschmann 2010) always increases from pith to  
317 bark (Kojima et al 2009, Koubaa et al 1998) until a distance considered as the limit of juvenile  
318 wood. For softwoods, the “typical radial pattern” for mechanical factors (Lachenbruch et al  
319 2011) is always the case for fast-growing plantations. It is characterized by a decrease of *RW*  
320 and an increase of both *SG* and *SM* from pith to bark until a juvenile core limit. For hardwoods  
321 this is not always the case, and *SG* can be more or less flat (Bendtsen & Senft 1986, while *SM*  
322 can be high near the pith and decrease for trees growing in dense tropical forest (Mc Lean et al  
323 2011).

324 There are few published results relating to radial variations of mechanical parameters in large  
325 trees of high forests that are not the result of plantation. Plourde et al (2015) studied radial  
326 density variation for 91 tropical species (Costa Rica). 42 over 74 had a net variation in density,  
327 37 with increasing TRP type and 5 with decreasing “anti TRP” type. Secondary forest species  
328 (open environment in juvenile phase) had the clearest positive variations (low juvenile density),

329 primary forest species (closed environment in juvenile phase) were the only anti-TRP species  
330 with a lower variation (high internal density). This is similar to what was found in French  
331 Guiana (Mc Lean et al 2011). On *Bagassa guianensis*, a fast-growing secondary forest tree of  
332 French Guiana, Bossu et al (2018) observed a general TRP pattern for AMF and density, very  
333 clear for density (0.3 to 0.9 along the radius). In addition, they identified a TRP pattern for  
334 interlocked grain: low in the inner zone and then increasing sharply towards the bark, resulting  
335 in a net increase in splitting fracture energy. Longuetaud et al (2017) studied 3 broadleaved  
336 trees: oak, beech, sycamore maple and two softwoods: fir and Douglas fir. The TRP model was  
337 valid for maple and Douglas fir, but for oak the density decreased instead of increasing. For fir  
338 and beech, the profile was bell-shaped (beech) or U-shaped (fir) with slight variations. Purba et  
339 al (2021) studied density and AMF in oak and beech for dominated, small-diameter trees  
340 harvested in thinning. Overall, the TRP applies to both cases

341 Authors measuring mechanical properties generally do not take into account the specific  
342 modulus, which is highly correlated with AMF, but being less noisy yields stronger statistical  
343 relationships ( $R^2$ ).

344 In Europe, old growth beech forests can have different forest origins: i) even-aged (France or  
345 Germany) or uneven-aged high forest (Switzerland), coppicing with standards (France) or  
346 conversion of coppice forest into high forest (Ciancio et al 2006) (Germany, France) but are  
347 very rarely the result of plantations (none in the 9 plots). *Fagus* is known for its shade tolerance  
348 and ability to grow very slowly under a closed canopy (Collet et al 2011) and most forest plots  
349 undergo more or less severe thinning before final harvesting, which leads to an increase of *RW*  
350 due to better access to light (Noyer et al 2017). This is reflected in the different mean *RW* radial  
351 patterns for the 9 plots (Fig. 9). For plots 7 (uneven-aged high forest) and 9 (middle forest  
352 transformed in even-aged high forest), a clear increase of *RW* is observed in the young ages,  
353 while the reverse and classical pattern is true for plots 1, 4, 5 and 6 (all even-aged forest in flat  
354 area). Similar results were found on younger beech trees (Bouriaud et al 2004). The low *RW*  
355 values for plots 2 and 8 (even aged, steep terrain) can be expected in a mountainous area, and  
356 the observed increase of *RW* after an initial decrease possibly due to thinning operations.

357 The lack of visible difference in mechanical properties between red and white beech wood  
358 confirms the observations by Pöhler et al (2006).

## 359 **6. Conclusion**

360 As a mean for these high forest beech trees, the radial patterns of variations are partly similar  
361 to the typical radial pattern for *RW* and *SM*. *SG* has a very small decreasing variation. But  
362 looking tree by tree, there are all types of patterns (increasing or decreasing at the beginning)  
363 for all parameters (*RW*, *SG* and *SM*). This supports the hypothesis of an “acclimation” for  
364 “mechanical” juvenility.

365 There is a very significant influence of forest plot on the 3 mechanical parameters sharing  
366 around 15% of the variance for each of them. The biggest sharing of variance comes from tree  
367 within the plot with a significant influence of the radial position (20 cm diameter core).

368 Due to the very low variability of the *SG* of beech wood, the variations of *SM* are much more  
369 important than those of *SG* in order to explain the variations of *MOE*.

## 370 **Acknowledgments**

371 The data were obtained thanks to the support of European Commission through the FAIR-  
372 project CT 98-3606, coordinated by Prof. Gero Becker. The financial support of CNRS K. C.  
373 Wong post-doctoral program and China Scholarship Council must be also acknowledged.



374 **References**

- 375 Alméras T, Thibaut A, Gril J. 2005. Effect of circumferential heterogeneity of wood maturation  
376 strain, modulus of elasticity and radial growth on the regulation of stem orientation in trees.  
377 *Trees* 19 (4), 457-467. <https://doi.org/10.1007/s00468-005-0407-6>
- 378 Alméras T, Clair B. 2016. Critical review on the mechanisms of maturation stress generation  
379 in trees. *Journal of the Royal Society, Interface* 13(122), 20160550.  
380 <https://doi.org/10.1098/rsif.2016.0550>
- 381 Bao FC, Jiang ZH, Jiang XM, Lu XX, Luo XQ, Zhang SY. 2001. Differences in wood  
382 properties between juvenile wood and mature wood in 10 species grown in China. *Wood*  
383 *Science and Technology* 35:363-375. <https://doi.org/10.1007/s002260100099>
- 384 Bhat KM, Priya PB, Rugmini P. 2001. Characterisation of juvenile wood in teak. *Wood Science*  
385 *and Technology* 34:517-532. <https://doi.org/10.1007/s002260000067>
- 386 Becker G, Beimgraben T. 2001. Occurrence and relevance of growth stresses in Beech (*Fagus*  
387 *sylvatica* L.) in Central Europe. Final Report of FAIR-project CT 98-3606, Coordinator Prof.  
388 G. Becker, Institut für Forstbenutzung und forstliche Arbeitwissenschaft, Albert-Ludwigs  
389 Universität, Freiburg, Germany.
- 390 Bendtsen BA, Senft J. 1986. Mechanical and anatomical properties in individual growth rings  
391 of plantation-grown eastern cottonwood and Loblolly pine. *Wood and Fiber Science* 18(1): 23-  
392 38.
- 393 Bossu J, Lehnebach R, Corn S, Regazzi A, Beauchene J, Clair B. 2018. Interlocked grain and  
394 density patterns in *Bagassa guianensis*: changes with ontogeny and mechanical consequences  
395 for trees. *Trees - Structure and Function*, 32(6):1643-1655. <https://doi.org/10.1007/s00468-018-1740-x>.
- 397 Bouriaud O, Bréda N, Le Moguédec G, Nepveu G. 2004. Modelling variability of wood specific  
398 gravity in beech as affected by ring age, radial growth and climate. *Trees* 18:264–276.  
399 <https://doi.org/10.1007/s00468-003-0303-x>
- 400 Brancheriau L, Baillères H. 2002. Natural vibration analysis of wooden beams: a theoretical  
401 review. *Wood Science and Technology*, 36(4):347-365. <https://doi.org/10.1007/s00226-002-0143-7>
- 403 Ciancio O, Corona P, Lamonaca A, Portoghesi L, Travaglini D. 2006. Conversion of clearcut  
404 beech coppices into high forests with continuous cover: A case study in central Italy. *Forest*  
405 *Ecology and Management* 224: 235–240. <https://doi.org/10.1016/j.foreco.2005.12.045>
- 406 Collet C, Fournier M, Ningre F, Hounzandji AP, Constant T. 2011. Growth and posture control  
407 strategies in *Fagus sylvatica* and *Acer pseudoplatanus* saplings in response to canopy  
408 disturbance. *Annals of Botany* 107, 1345–1353. <https://doi.org/10.1093/aob/mcr058>
- 409 Cown D, Dowling L. 2015. Juvenile wood and its implications. *NZ Journal of Forestry*,  
410 February 2015, Vol. 59, No. 4: 10-17
- 411 Déjardin A, Laurans F, Arnaud D, Breton C, Pilate G, Leplé JC. 2010. Wood formation in  
412 Angiosperms. *C. R. Biologies* 333 (2010) 325–334
- 413 Jullien D, Widmann R, Loup C, Thibaut B. 2013. Relationship between tree morphology and  
414 growth stress in mature European beech stands. *Annals of forest science* 70 (2), 133-142.  
415 <https://doi.org/10.1007/s13595-012-0247-7>
- 416 Kojima M, Yamamoto H, Yoshida M, Ojio Y, Okumura K. 2009. Maturation property of fast-  
417 growing hardwood plantation species: A view of fiber length. *Forest Ecology and Management*  
418 257: 15–22. <https://doi.org/10.1016/j.foreco.2008.08.012>
- 419 Koubaa A, Hernandez RE, Baudouin M, Poliquin J. 1998. Inter clonal, intra clonal and within-  
420 tree variation of fiber length of poplar hybrid clones. *Wood and Fiber Science* 30(1): 40-47

421 Kretschmann DE. 2010. Mechanical properties of wood. In Wood handbook: Wood as an  
422 engineering material. General Technical Report FPL-GTR-190. Madison: Forest Products  
423 Laboratory, USDA, Forest Service.

424 Lachenbruch B, Moore J, Evans R. 2011. Radial variation in wood structure and function in  
425 woody plants, and hypotheses for its occurrence. In: Meinzer FC, Lachenbruch B, Dawson TE  
426 (eds) Size- and age-related changes in tree structure and function. Springer, Dordrecht: 121–  
427 164.

428 Longuetaud F, Mothe F, Santenoise P, Diop N, Dlouha J, Fournier M, Deleuze C. 2017. Patterns  
429 of within-stem variations in wood specific gravity and water content for five temperate tree  
430 species. *Annals of Forest Science* 74:64. <https://doi.org/10.1007/s13595-017-0657-7>

431 Loup C, Fournier M, Chanson B. 1991. Relations entre architecture mécanique et anatomie de  
432 l'arbre : cas d'un Pin Paritime (*Pinus pinaster* Soland.). *L'arbre, biologie et développement*.  
433 *Naturalia monspeliensa* N° hors série (C. Edelin ed)

434 Liu S, Loup C, Gril J, Dumonceaud O, Thibaut A, Thibaut B. 2005. Studies on European beech  
435 (*Fagus sylvatica* L.): variations of colour parameters. *Annals of Forest Science*, 62: 625-632.  
436 <https://doi.org/10.1051/forest:2005063>

437 Mc Lean JP, Zhang T, Bardet S, Beauchêne J, Thibaut A, Clair B, Thibaut B. 2011. The  
438 decreasing radial wood stiffness pattern of some tropical trees growing in the primary forest is  
439 reversed and increases when they are grown in a plantation. *Annals of Forest Science* 68: 681-  
440 688. <https://doi.org/10.1007/s13595-011-0085-z>

441 Noyer E, Lachenbruch B, Dlouhá J, Collet C, Ruelle J, Ningre F, Fournier M. 2017. Xylem  
442 traits in European beech (*Fagus sylvatica* L.) display a large plasticity in response to canopy  
443 release. *Annals of Forest Science* 74: 46, <https://doi.org/10.1007/s13595-017-0634-1>

444 Plourde BT, Boukili VK, Chazdon RL. 2015. Radial changes in wood specific gravity of  
445 tropical trees: inter- and intraspecific variation during secondary succession. *Functional*  
446 *Ecology*, 29:111–120. <https://doi.org/10.1111/1365-2435.12305>

447 Pöhler E, Klingner R, Künniger T. 2006. Beech (*Fagus sylvatica* L.) – Technological properties,  
448 adhesion behaviour and colour stability with and without coatings of the red heartwood. *Ann.*  
449 *For. Sci.* 63 (2006) 129-137. <https://doi.org/10.1051/forest:2005105>

450 Purba CYC, Dlouha J, Ruelle J, Fournier M. 2021. Mechanical properties of secondary quality  
451 beech (*Fagus sylvatica* L.) and oak (*Quercus petraea* (Matt.) Liebl.) obtained from thinning,  
452 and their relationship to structural parameters. *Annals of Forest Science* 78: 81.  
453 <https://doi.org/10.1007/s13595-021-01103-x>

454 R Core Team 2018. R: A language and environment for statistical computing. R Foundation for  
455 Statistical Computing, Vienna, Austria.

456 Raven PH, Evert RF, Eichhorn SE. 2007. *The biology of plants*. Brussels: De Boeck.

457 Savidge RA. 2003. Tree growth and wood quality. In: *Wood quality and its biological basis*,  
458 edited by JR. Barnett and G. Jeronimidis, Blackwell scientific, Oxford, UK (ISBN: 978-1-405-  
459 14781-1): 1-29

460 Sorz J, Hietz P. 2008. Is oxygen involved in beech (*Fagus sylvatica*) red heartwood formation?  
461 *Trees* 22:175–185. <https://doi.org/10.1007/s00468-007-0187-2>

462 Thibaut B. 2019. Three-dimensional printing, muscles and skeleton: mechanical functions of  
463 living wood. *Journal of Experimental Botany*, Volume 70, Issue 14, 1 July 2019, Pages 3453–  
464 3466. <https://doi.org/10.1093/jxb/erz153>

465 Thibaut B, Gril J. 2021. Tree growth forces and wood properties. *Peer Community Journal*,  
466 Volume 1, article no. e46. <https://doi.org/10.24072/pcjournal.48>

467 Trenčiansky M, Lieskovský M, Merganič J, Šulek R. 2017. Analysis and evaluation of the  
468 impact of stand age on the occurrence and metamorphosis of red heartwood. iForest, 10: 605-  
469 610. <https://doi.org/10.3832/ifor2116-010>

470 Wernsdörfer H, Constant T, Mothe F, Badia MA, Nepveu G, Seeling U. 2005. Detailed  
471 analysis of the geometric relationship between external traits and the shape of red heartwood in  
472 beech trees (*Fagus sylvatica* L.). Trees 19: 482–491. <https://doi.org/10.1007/s00468-005-0410->  
473 [y](https://doi.org/10.1007/s00468-005-0410-y)